journal

J. Am. Ceram. Soc., 77 [2] 499–504 (1994)

Infiltration of Reaction-Bonded Silicon Nitride with Equilibrium Y-Si-O-N Melt

Tzer-Shin Sheu*

Department of Biologic and Materials Science, School of Dentistry, The University of Michigan, Ann Arbor, Michigan 48109-1078

An equilibrium Y-Si-O-N melt was infiltrated to eliminate the open porosity of reaction-bonded silicon nitride at 1600–1800°C. This oxynitride melt contained two equilibrium phases, a β-Si_3N_4 solid phase and a liquid phase at high temperatures. Before infiltration, porous reaction-bonded silicon nitride compacts were heat-treated to completely transform to the β-Si_3N_4 phase. After infiltration, the flexural strength of the reaction-bonded silicon nitride material increased from 200 to 600 MPa at 25°C, from 200 to 300 MPa at 1400°C in air.

I. Introduction

THROUGH a gas-nitriding process to transform a porous silicon compact into reaction-bonded silicon nitride (RBSN), a net-shape of silicon nitride ceramic has been fabricated with a linear dimension error of less than 0.05%.[1,2] The flexural strength of this reaction-bonded material is temperature-independent at 25–1600°C.[3–5] Even with such precise fabrication, this high-temperature structural material is lacking in excellent mechanical properties and oxidation resistance at high temperatures because of its approximately 10–20 vol% remaining porosity.[6] In the past, several methods such as metallic infiltration[7] and postsintering techniques[8–10] have been introduced to eliminate the remaining porosity. However, most of these methods have destroyed the self-bonded Si_3N_4 skeleton structure or have changed the dimensions of the RBSN material. In this study, a modified melt infiltration method has been chosen to eliminate the open porosity and to maintain the self-bonded Si_3N_4 interconnected structure.

In this modified melt infiltration, a melt which contains two equilibrium phases at high temperatures is designed to infiltrate into the RBSN. By establishing a phase equilibrium condition between the liquid and the pure silicon nitride solid phase in the melt, the liquid will not chemically react with the RBSN during infiltration. This modified melt infiltration method is expected to be much easier to handle than the conventional method, because the limiting factors such as temperature and time[7,11] will not have to be considered. The oxynitride melt is chosen from the Y-Si-O-N quaternary system. In this quaternary system, pure Si_3N_4 solid phase is phase equilibrated with the liquid in the Si_3N_4–$Y_2Si_2O_7$–$Y_5(SiO_4)_3N$ triangle at 1500°C as shown in Fig. 1.[12] As temperature increases, this liquid is extended to the Si_3N_4–$Y_2Si_2O_7$ line. In considering the high-temperature mechanical properties of the infiltrated RBSN material, the composition of the oxynitride melt is chosen along the Si_3N_4–$Y_2Si_2O_7$ line instead of the composition inside the Si_3N_4–$Y_2Si_2O_7$–$Y_5(SiO_4)_3N$ triangle.

Most of the as-received RBSN materials contain two polymorphs, α- and β-Si_3N_4. However, in the oxynitride melt, the liquid is phase equilibrated with the β-Si_3N_4. When this oxynitride melt is infiltrated to the RBSN materials, the α-Si_3N_4 phase in the RBSN materials is probably dissolved in the infiltrated liquid and then reprecipitated in the β-Si_3N_4 phase. In order to maintain the self-bonded Si_3N_4 interconnected structure in the infiltrated RBSN materials, the as-received RSBN is heat-treated to completely transform to the β-Si_3N_4 phase before infiltration. Pore size distributions and dimension changes of the RBSN materials were observed before and after post-heat treatments. Furthermore, after infiltration, microstructure and high-temperature mechanical properties of the infiltrated RBSN materials were investigated.

II. Experimental Procedure

Starting powders for making oxynitride melts were 99.9% pure Si_3N_4 (containing ~95% α and ~5% β), 99.99% pure Y_2O_3, and 99.99% pure SiO_2 (low quartz). According to the composition of 70 equiv% Si–30 equiv% Y as indicated in Fig. 1 by the symbol "*", these three powders were attrition-milled with 99.99% pure isopropyl alcohol. After the isopropyl alcohol was removed, these dried powders were fired at 1600–2000°C under 25 atm of N_2 to form oxynitride melts. Subsequently, these premelted oxynitride melts were cooled down to room temperature to determine their phase existence and then prepared for infiltration at high temperature.

Two sources of the reaction-bonded silicon nitride materials were used in this study. One was from Ceradyne Inc., and it contained 67 wt% α-Si_3N_4 and 33 wt% β-Si_3N_4, determined by an X-ray diffraction method.[13] The other was synthesized in this laboratory from 99.99% pure silicon powder having a median

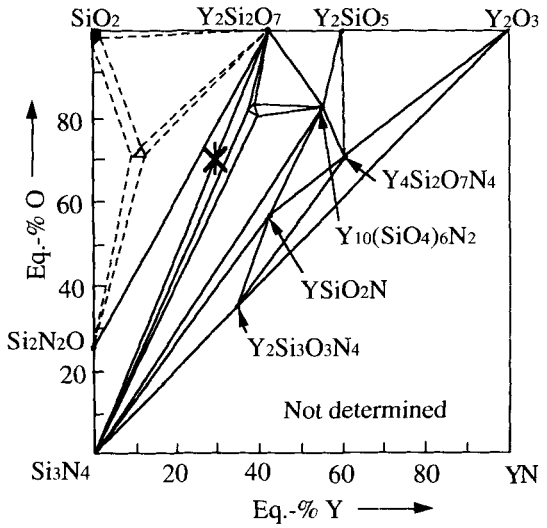

Fig. 1. Isothermal phase relationships at 1500°C in the Si-Y-O-N quaternary system (Ref. 12). "*" indicates a composition with 30 equiv% Y–70 equiv% Si along the Si_3N_4–$Y_2Si_2O_7$ line.

R. Rice—contributing editor

Manuscript No. 194716. Received April 2, 1993; approved October 29, 1993.

particle size of ~1 μm. These pure silicon powders were hot-pressed by a uniaxial compressive stress of 26 MPa to form a porous compact at 1200°C under 1 atm of flowing Ar gas. Subsequently, this partially sintered silicon compact was gas-nitrided to form reaction-bonded silicon nitride. These two sources of RBSN materials were further post-heat-treated at 1600°–1900°C under 25 atm of N_2 to enable them to completely transform to the β-Si_3N_4 phase. Heat treatments of these RBSN materials are listed in Table I. A mercury porosimeter was used to analyze the pore size distributions of the RBSN materials before and after heat treatments.

The premelted oxynitride melts were placed over the post-heat-treated RBSN compacts and were then one-dimensionally vertically infiltrated to these RBSNs at 1600–1800°C under 25 atm of N_2. After infiltration, some of the infiltrated RBSN materials were heat-treated at 1400°C for a crystallization treatment. The mechanical properties of these RBSN materials were tested at 25–1400°C in the air by a four-point SiC bending fixture. The inner and outer spans of the bending fixture were 8 and 16 mm, respectively. The dimension of the testing bar was 25 × 3 × 2 mm^3. The testing strain rate was 1 × 10^{-4}/s. The specimen's surfaces were polished and its sharp edges were also chamfered by a diamond paste down to 1 μm. Microstructural observations were conducted either by SEM or by TEM. The phase existence of the oxynitride melts and the RBSN materials at high temperature was determined by the X-ray diffraction technique at room temperature.

III. Results and Discussion

(1) Preparations of Oxynitride Melts and RBSN Materials for Infiltration

An oxynitride melt with the initial composition 30 equiv% Y–70 equiv% Si was premelted at high temperatures under different N_2 pressures. Under low pressure, i.e., 1–2 atm of N_2, this melt had considerable weight loss, approximately 30 wt% after being fired at 1700°C for 1 h. The corresponding X-ray diffraction pattern shows that this fired oxynitride melt contains only the $Y_{10}(SiO_4)_6N_2$ apatite phase without any detectable glass background. This decomposition phenomenon indicates that the final composition of the oxynitride melt is more likely to shift to the $Y_{10}(SiO_4)_6N_2$ corner. The weight loss of this oxynitride melt is probably caused by the formation of SiO and N_2, which is one of the decomposition mechanisms in silicon nitride-containing materials.[14]

However, there is no weight loss for this 30 equiv% Y–70 equiv% Si oxynitride melt after being fired at 1700–2000°C under 25 atm of N_2. The series of corresponding X-ray diffraction patterns presented in Fig. 2 indicate this oxynitride melt contains a β-Si_3N_4 phase and a liquid at 1700° and 1850°C, and only a liquid at 2000°C. All of the X-ray diffraction patterns shown in Fig. 2 were determined at room temperature. The characteristic X-ray background of the liquid phase, which is an oxynitride glass at room temperature, appears from 2θ = ~22° to 2θ = ~38° in these diffraction patterns. The above phase relationships indicate that the liquidus gradually approaches the Si_3N_4 corner as temperature increases. At higher temperature (≥2000°C), this 30 equiv% Y–70 equiv% Si oxynitride melt does not contain a liquid in equilibrium with the β-Si_3N_4 phase and it will chemically react with the RSBN during infiltration. However, at 1600–1800°C, this oxynitride melt contains a liquid in equilibrium with the β-Si_3N_4 phase and it will not chemically react with the RSBN during infiltration. Therefore, this 30 equiv% Y–70 equiv% Si oxynitride melt is chosen to infiltrate into the RBSN at 1600–1800°C. Table I lists the phase existence, dimension change, and porosity of the post-heat-treated Ceradyne RBSNs (samples A1–A9) and samples B0–B2. As-received RBSNs from Ceradyne are heat-treated at 1600–1900°C under 25 atm of N_2. The minimum temperature to obtain a single β-Si_3N_4 phase is ~1650°C. With a low-temperature heat treatment, it takes a longer time to complete this α-Si_3N_4-to-β-Si_3N_3 phase transformation, which is >5 h at 1650°C, but <0.25 h at 1900°C; however, the linear dimension change (ΔL) of this heat-treated RBSN is smaller, i.e., ~1% at 1650°C for sample A5 versus ~3.0% at 1900°C for sample A8. As to the porosity (V_p) and median pore size (d_m), the heat-treated RBSN sample has a lower porosity but a larger median pore size than the as-received RBSN. For a group of RBSNs

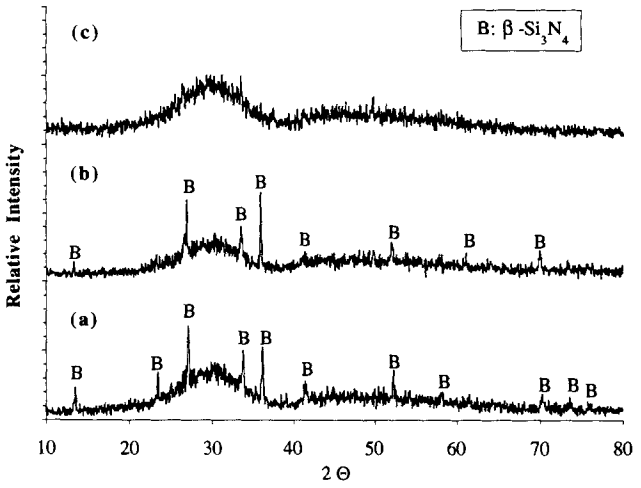

Fig. 2. X-ray diffraction patterns of the Y-Si-O-N melts with the composition 30 equiv% Si–70 equiv% Y fired at (a) 1700, (b) 1850, and (c) 2000°C. X-ray diffraction patterns are determined at room temperature after these samples are rapidly cooled from high temperatures.

Table I. Phase Existence, Dimension Change, Density, and Porosity of the Silicon Compact and the Reaction-Bonded Silicon Nitride Materials before and after Heat Treatment

Sample	Post-heat-treatment (referred to A1 and B1)	β-Si_3N_4 (wt%)	ΔL* (%)	D_b† (g/cm^3)	D_s† (g/cm^3)	D_t§ (g/cm^3)	V_{op}¶ (vol%)	V_{cp}** (vol%)	V_p†† (vol%)	Median pore size d_m (μm)
A1	As-received RBSN	33	r.f.	2.255	2.904	3.186‡‡	20.4	9.7	30.1	0.085
A2	1600°C, 2.5 h	48	~0							
A3	1600°C, 15 h	74	~0							
A4	1650°C, 5 h	73	~−1							
A5	1650°C, 10 h	100	~−1	2.375	3.141	3.192‡‡	24.0	1.6	25.6	0.526
A6	1700°C, 5 h	100	~−1.7							
A7	1800°C, 2 h	100	~−2.6							
A8	1900°C, 0.25 h	100	~−3.0	2.432	3.076	3.192‡‡	20.2	3.6	23.8	0.395
A9	1900°C, 2 h	100	~−3.0	2.497	3.173	3.192‡‡	21.2	0.6	21.8	1.079
B0	Silicon compact		r.f.	1.700	2.289	2.329§§	25.3	1.7	27.0	0.356
B1	RBSN from B0	38	~0	2.661	3.086	3.186‡‡	13.3	3.1	16.4	0.118
B2	1900°C, 1 h	100	~−0.5	2.699	3.062	3.192‡‡	11.4	4.1	15.5	0.531

*Linear dimension change. †Bulk density. ‡Skeleton density (including close pore). §Theoretical density. ¶Volume fraction of the open porosity. **Volume fraction of the closed porosity. ††Total porosity. ‡‡Data calculated from Ref. 17. §§Data from JCPDs 27-1402.

(Al, A8, and A9), Table I shows the median pore size increases as the time of heat treatment increases. Two corresponding SEM micrographs presented in Fig. 3 show a larger hexagon prism type of β-Si_3N_4 grains in the single β-Si_3N_4 phase containing RBSN, in contrast to a very fine two-phase microstructure, a needlelike grain, and an equiaxial type of grain in the as-received RBSN. Apparently, the median pore size in the heat-treated RBSNs is affected by the β-Si_3N_4 grain growth; that is, the median pore size increases as the β-Si_3N_4 grain size increases.

Sample B0–B2 in Table I represent one example of a series of heat treatments from silicon compact to RBSN, and further to a single β-Si_3N_4 phase containing RBSN. As to the heat treatment from the silicon compact to the RBSN, there is no dimension change (ΔL = ~0) between samples B0 and B1. This result is consistent with previous studies.[1,2] A direct conversion of silicon to silicon nitride usually causes a volume increase of ~22%, which can be calculated from the molecular weights and the theoretical densities (D_t) of silicon and silicon nitride as listed in Table I. However, this is not the case for the heat treatment from the silicon compact to the RBSN. The heat treatment from the silicon compact to the RBSN only causes an internal structure change instead of an external dimension change. A porosity change from 27.0 to 16.4 vol% and a median pore size change from 0.356 to 0.118 μm for samples B0 and B1 are examples of this internal structure change. During transformation, part of the silicon nitride is probably formed to fill in the preexisting empty space, which was a pore in the silicon compact before transformation. As a result, RBSN has a lower porosity and a smaller median pore size. As to the further heat treatment from the RBSN to a single β-Si_3N_4 phase containing RBSN, there is no significant dimension change (ΔL = ~0.5%) or porosity (V_p = ~16 vol%) difference for samples B1 and B2. However, as a result of the β-Si_3N_4 grain growth in sample B2, the median pore size increases from 0.118 to 0.531 μm. Overall, the phenomena being observed during these series of heat treatments can be summarized as follows: the median pore size decreases first because of the formation of silicon nitride, and then increases because of β-Si_3N_4 grain growth; however, the dimension change between the initial and final products is not significant (ΔL = ~0.5%). As a result, a net-shape of the infiltrated silicon nitride ceramic can be precisely fabricated with a linear dimension error <0.5% in this modified melt infiltration method.

(2) Infiltration of Oxynitride Melt into the RBSN Compact

Figure 4(a) shows a typical microstructure of the oxynitride melt for this modified melt infiltration. There are two phases in this oxynitride melt, the elongated grains of β-Si_3N_4 phase and a bright background of glass matrix which is a liquid at high temperature. When the oxynitride melt is infiltrated to a single β-Si_3N_4 containing RBSN at high temperature, the liquid is automatically "capillary-flowed" into the RBSN compact; however, β-Si_3N_4 grains are too large to pass through the interconnected pore channel in the RBSN compact and therefore they are left behind in the interface. This phenomenon can be seen in Fig. 4(b), in which β-Si_3N_4 grains are sedimented in the interface between the RBSN compact and the oxynitride melt.

The relationship of the infiltration depth versus time is presented in Fig. 5. The infiltration depth (d) is linearly proportional to the square root of time ($t^{1/2}$) for melt infiltration at 1700°C. That is, $d^2 = kt$, k being a constant which is proportional to the fluidity (1/viscosity).[15] From this parabolic relationship of infiltration depth versus time, the infiltration mechanism of the oxynitride melt into the RBSN material is capillary flow,[11,15] not a chemical reaction or surface desorption.[16] A positive intercept of infiltration depth at time = 0 occurs probably because the liquid in the oxynitride glass is already formed and then infiltrated into the RBSN compact before the temperature reaches 1700°C. The infiltration depth is also temperature-dependent. Data points presented in Fig. 5 indicate that the infiltration depth at 1700°C is larger than that at 1600°C, but smaller than that at 1800°C. A larger infiltration depth at high temperature is obtained because the lower viscosity of the liquid in the oxynitride melt generates a larger infiltration constant (k) in this capillary flow infiltration. This capillary flow mechanism further confirms a phase compatibility between the oxynitride melt and the RBSN during infiltration.

(3) High-Temperature Mechanical Properties and Microstructural Observations

The flexural strength of the RBSN materials before and after infiltration is shown in Fig. 6. The processing conditions of these tested RBSN materials are listed in Table II. The flexural strength of sample A1 is 200 MPa and it is temperature-independent at 25–1400°C, which is consistent with previous studies.[18] As to the post-heat-treated RBSN sample A9, which contains 100% β-Si_3N_4, its flexural strength is ~200 MPa and it is temperature-independent at 25–1400°C. It indicates that the

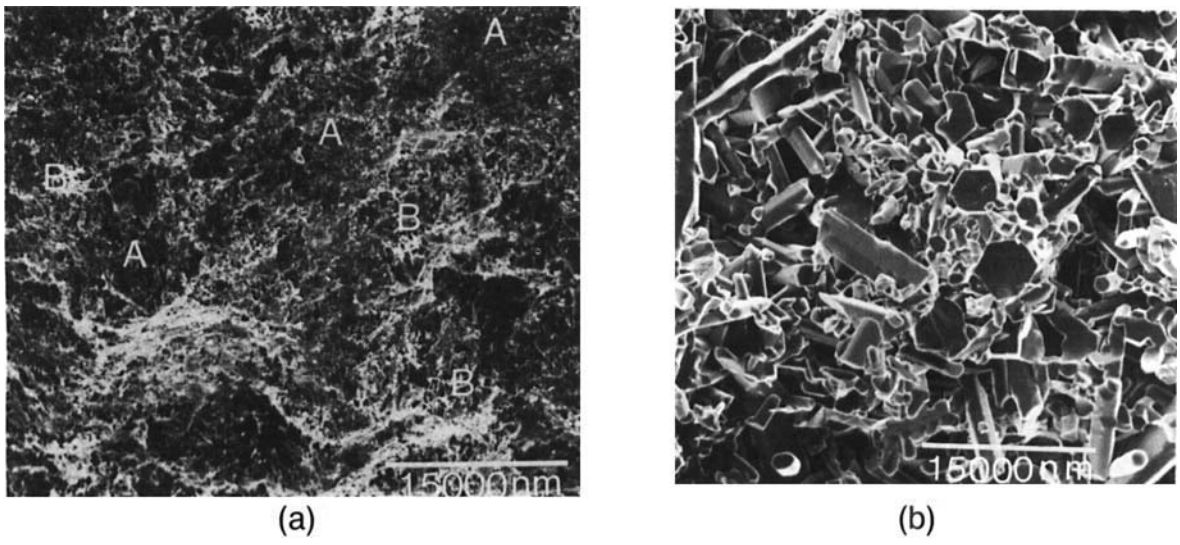

Fig. 3. SEM micrographs of (a) as-received RBSN from Ceradyne and (b) a single β-Si_3N_4 phase containing RBSN. As-received RBSN from Ceradyne contains two different microstructures, an equiaxial grain (marked by symbol A) and a needlelike grain (marked by symbol B). A single β-Si_3N_4 phase containing RBSN contains a hexagon prism type of β-Si_3N_4 grains. This specimen has been heat-treated at 1900°C for 2 h under 25 atm of N_2.

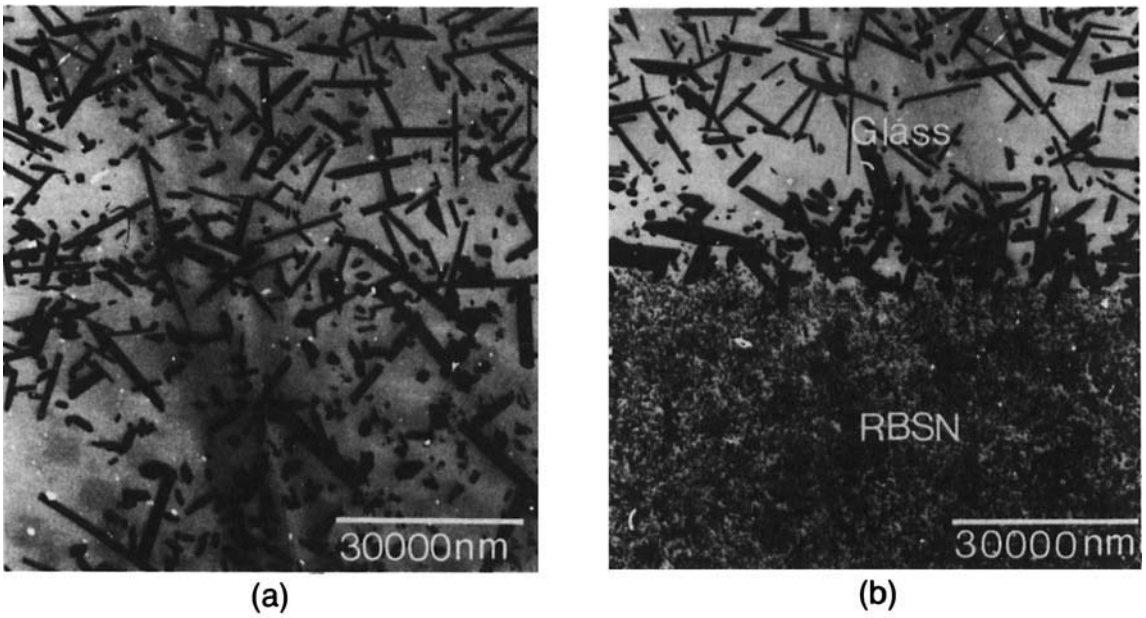

Fig. 4. SEM micrographs of (a) an oxynitride melt for infiltration and (b) the interface between the RBSN and oxynitride melt during infiltration. The elongated β-Si_3N_4 grains are sedimented in the interface.

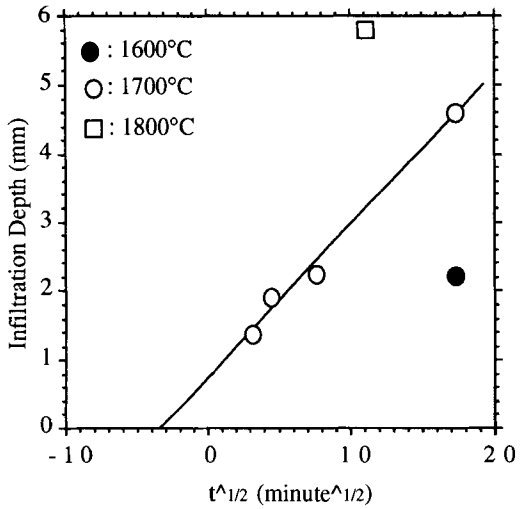

Fig. 5. Relationship of infiltration depth (d) versus square root of time ($t^{1/2}$) for the RBSNs infiltrated at different temperatures. These RBSN samples have been heat-treated at 1900°C for 2 h before infiltration.

formation of the elongated β-Si_3N_4 phase does not degrade the mechanical properties of the RBSN materials. In Fig. 6, all of the infiltrated RBSNs except for sample D1640 have better mechanical properties than the as-received RBSN. The maximum flexural strength of the infiltrated RBSNs is increased from 200 to 600 MPa at 25°C, and from 200 to 300 MPa at 1400°C. SEM fractographs presented in Fig. 7 show some β-Si_3N_4 grain pull-outs in these tested samples which are represented by sample D1790, but not for sample D1640 at 1400°C. Sample D1640 has a very low flexural strength of ~50 MPa at 1400°C. The low mechanical properties of this sample at high temperature occur probably because its microstructure is different from the other infiltrated RBSNs. Sample D1640 has a microstructure where the β-Si_3N_4 grains are dispersed in an oxynitride glass matrix, because the self-bonded Si_3N_4 skeleton structure is destroyed by an α-Si_3N_4-to-β-Si_3N_4 phase transformation during infiltration. However, the other infiltrated RBSNs have microstructures where the two continuous phases, β-Si_3N_4 and oxynitride glass, are interwoven to form a three-dimensional composite. Compared to the three-dimensional composite microstructure of the other infiltrated RBSN, sample D1640 is expected to have low mechanical properties at 1400°C because during a mechanical test the cracks are likely to propagate along the weak glass phase instead of through the hard β-Si_3N_4 phase.

The infiltrated RBSN materials with and without a subsequent crystallization treatment are represented by samples D169C and D1690, respectively. From X-ray diffraction, sample D1690 is determined to contain only one crystalline phase β-Si_3N_4, but in sample D169C there are three crystalline phases—β-Si_3N_4, $Y_2Si_2O_7$, and a minor apatite ($Y_{10}(Si_4)_6N_2$) phase. The phase difference in these two samples occurs because sample D169C has an additional crystallization treatment at 1400°C for 10 h. The presence of the minor apatite ($Y_{10}(Si_4)_6N_2$) phase in sample D169C indicates that the composition of the infiltrated oxynitride liquid is a little off the Si_3N_4–

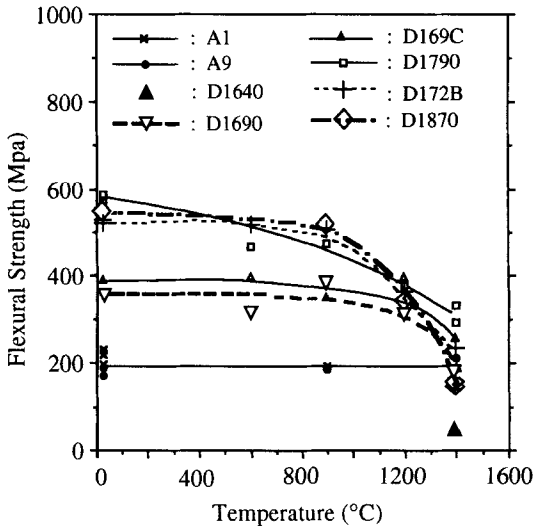

Fig. 6. Flexural strength of the RBSN materials tested at 25–1400°C in the air. The processing conditions of these tested specimens are listed in Table II.

Table II. Processing Conditions of the Infiltrated Reaction-Bonded Silicon Nitride Materials as Listed in Fig. 7

Sample	RBSNs for infiltration*	Temperature for infiltration (°C)	Post-heat-treatment after melt infiltration
Al	A1	No	No
A9	A9	No	No
D1640	A4	1600	No
D1690	A9	1600	No
D169C	A9	1600	1400°C, 10 h
D1790	A9	1700	No
D172B	B2	1700	No
D1870	A7	1800	No

*Referred to Table I.

$Y_2Si_2O_7$ composition line. Compared to sample D1690, sample D169C does not have a significant improvement of mechanical properties as shown in Fig. 6. This is because the oxynitride glass in the infiltrated RBSN is not completely crystallized after a crystallization treatment at 1400°C for 10 h. The incomplete crystallization phenomenon of this sample can be seen from the SEM and TEM micrographs in Fig. 8, in which the crystalline structures in the glass pocket are surrounded by a continuous glass.

Mechanical properties of the infiltrated RBSNs are also affected by the infiltrated temperature. In Fig. 6, RBSNs infiltrated at 1600°C have lower flexural strength than those infiltrated at 1700° and 1800°C. The larger defects in the low-temperature infiltrated RBSNs may cause inferior mechanical properties because the higher viscosity liquid is unable to infiltrate into the smaller pores. Samples D172B and D1790 have similar mechanical properties even though RBSNs for these two samples are from different sources before infiltration. It seems that the mechanical properties of the infiltrated RBSNs are mainly controlled by the infiltrated temperature.

As listed in Table I, the post-heat-treated RBSNs contain ~1.0–~10.0 vol% of the closed porosity before infiltration. This closed porosity is unable to infiltrate with the liquid during infiltration, and it will all remain inside the samples to affect the mechanical properties. To optimize the mechanical properties of the infiltrated RBSNs, the amount of the closed porosity needs to be minimized. Furthermore, with infiltrating a higher meltpoint of glass and by conducting a complete crystallization treatment, the RBSN materials are expected to have better mechanical properties.

IV. Conclusion

(1) A modified melt infiltration method is introduced to eliminate the open porosity of the RBSN materials. In this infiltration method, the oxynitride melt which contains two equilibrium phases, a liquid and a β-Si_3N_4 phase, is infiltrated to the porous RBSN compact at high temperatures. In order to maintain the self-bonded Si_3N_4 interconnected structure during infiltration, the RBSN materials are heat-treated to completely

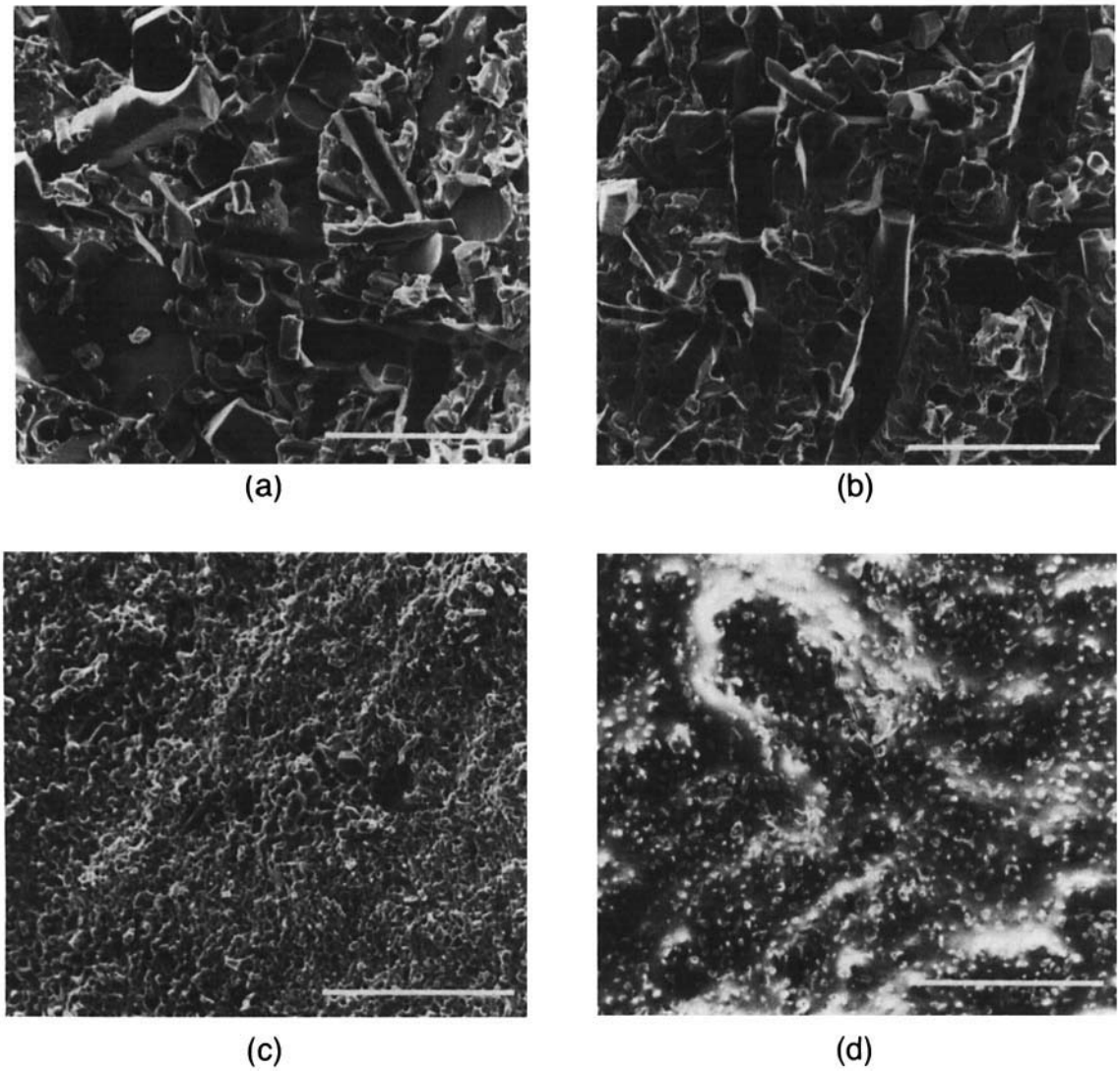

Fig. 7. SEM fractographs of the infiltrated RBSN samples (a) D1790 at 25°C, (b) D1790 at 1400°C, (c) D1640 at 25°C, and (d) D1640 at 1400°C. These samples are bend-tested at 25° and 1400°C in the air. Scale bars are 15 000 nm.

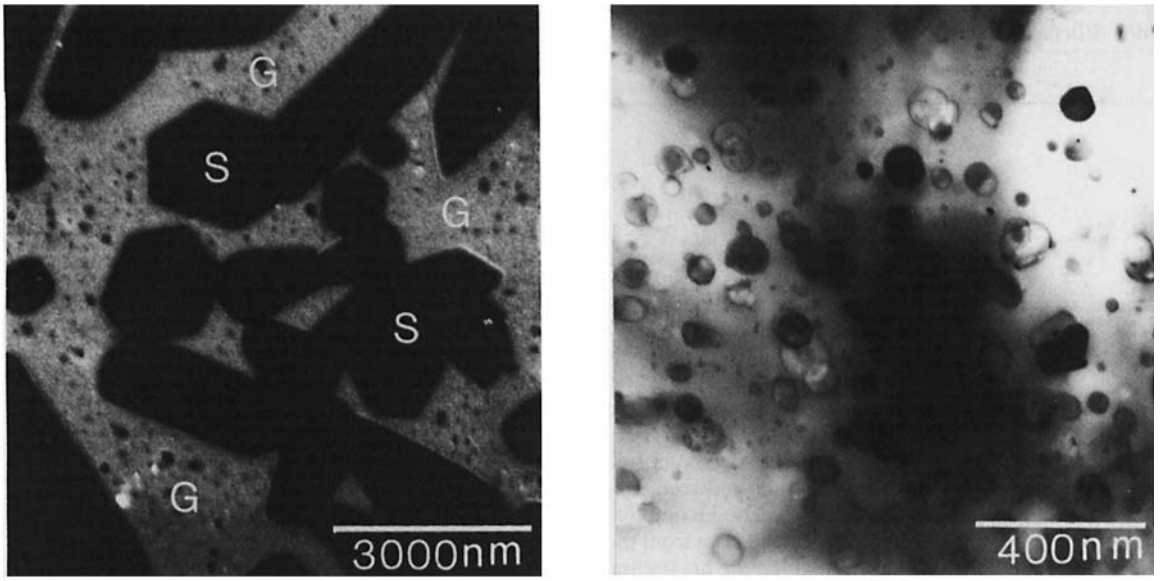

Fig. 8. Microstructure for sample D169C with a crystallization treatment at 1400°C for 10 h: (a) SEM micrograph, containing β-Si_3N_4 grains and oxynitride glass pockets, and (b) TEM micrograph, showing the distribution of crystallization structures in the oxynitride glass pocket. Symbol G is for oxynitride glass pockets; symbol S is for the β-Si_3N_4 grains.

transform to the β-Si_3N_4 phase before infiltration. By transforming the silicon compact into the RBSN, and further to a single β-Si_3N_4 containing RBSN, the median pore size in these materials is changed, increasing first and then decreasing; however, the dimension change among these materials can be very small (<0.5%).

(2) By establishing a phase equilibrium between the liquid and β-Si_3N_4 in the oxynitride melt, the infiltration mechanism of this oxynitride melt to a single β-Si_3N_4 phase containing RBSN is capillary flow,[11,15] not a chemical reaction or surface desorption.[16]

(3) Using this modified melt infiltration method, the mechanical properties of the RBSN materials are improved. Flexural strength increases from 200 up to 600 MPa at 25°C, and from 200 to 300 MPa at 1400°C. In order to further improve the mechanical properties of these infiltrated RBSN materials, it is suggested that the RBSN compact needs to first minimize its closed porosity before infiltration and then undergo a complete crystallization treatment after infiltration.

Acknowledgments: Special thanks to Dr. T. Y. Tien for his discussion and Mr. J. A. Mangels for the gift of the RBSN materials used in this study.

References

[1]D. J. Godfrey, "Ceramics for High-Temperature Engineering," *Proc. Br. Ceram. Soc.*, **22,** 1–25 (1973).

[2]D. J. Godfrey, "The Use of Ceramics in High-Temperature Engineering," *Met. Mater.*, **2,** 305 (1968).

[3]A. G. Evans and R. W. Davidge, "Strength and Oxidation of Reaction-Sintered Silicon Nitride," *J. Mater. Sci.*, **5** [4] 314–25 (1973).

[4]A. F. McLean, E. A. Fisher, and R. J. Bratton, "Brittle Materials Design, High Temperature Gas Turbine," AMMRC Interim Rept. Nos. 1–12 under Contract No. DAAG 46-71-CO162, 1972–1978.

[5]M. L. Torti, "The Silicon Nitride and Sialon Families of Structural Ceramics"; pp. 161–94 in Treatise on Materials Science and Technology, Vol. 29, *Structural Ceramics*. Edited by J. B. Wachtman, Jr. Academic Press, New York, 1989.

[6]J. C. Uy, "Instability of Reaction-Sintered Silicon Nitride," *Am. Ceram. Soc. Bull.*, **57** [8] 735–40 (1978).

[7]W. G. Schmidt, "Metallic Infiltration of Reaction Bonded Silicon Nitride"; pp. 447–53 in *Progress in Nitrogen Ceramics*. Edited by F. L. Riley. Martinus Nijhoff, The Hague, Netherlands, 1983.

[8]J. A. Mangels and G. J. Tennenhouse, "Densification of Reaction-Bonded Silicon Nitride," *Am. Ceram. Soc. Bull.*, **59** [12] 1216–22 (1980).

[9]H. H. Gasthuber, J. G. Heinrich, and J. A. Huber, "Hot Isostatically Pressed Reaction-Bonded Silicon Nitride Prechamers for the Diesel Engine," *Am. Ceram. Soc. Bull.*, **68** [12] 2104–108 (1989).

[10]H. J. Kleebe and G. Ziegler, "Influence of Crystalline Secondary Phases on the Densification Behavior of Reaction-Bonded Silicon Nitride During Post-sintering under Increased Nitrogen Pressure," *J. Am. Ceram. Soc.*, **72** [12] 2314–17 (1989).

[11]W. B. Hillig, "Melt Infiltration Approach to Ceramic Matrix Composites," *J. Am. Ceram. Soc.*, **71** [2] C-96–C-99 (1988).

[12]L. J. Gauckler, H. Hohne, and T. Y. Tien, "The System Si_3N_4–SiO_2–Y_2O_3," *J. Am. Ceram. Soc.*, **63,** 35–37 (1980).

[13]C. P. Gazzara and D. R. Messier, "Determination of Phase Content of Si_3N_4 by X-ray Diffraction Analysis," *J. Am. Ceram. Soc.*, **56** [9] 777–80 (1988).

[14]G. Leng-Ward and M. H. Lewis, "Oxynitride Glasses and Their Glass-Ceramic Derivatives"; pp. 106–55 in *Glasses and Glass-Ceramics*. Edited by M. H. Lewis. Chapman and Hall, London, U.K., 1989.

[15]E. W. Washburn, "The Dynamics of Capillary Flow," *Phys. Rev.*, **17,** 273–83 (1921).

[16]C. Toy and W. D. Scott, "Ceramic-Melt Composite Produced by Melt Infiltration," *J. Am. Ceram. Soc.*, **73** [1] 97–101 (1990).

[17]K. H. Jack, "The Characterization of α′-Sialons and the α-β Relationships in Sialons and Silicon Nitrides"; pp. 45–60 in *Progress in Nitrogen Ceramics*. Edited by F. L. Riley. Martinus Nijhoff, The Hague, Netherlands, 1983.

[18]J. R. G. Evans and A. J. Moulson, "Microstructure of Densified Reaction Bonded Silicon Nitride"; pp. 237–43 in *Progress in Nitrogen Ceramics*. Edited by F. L. Riley. Martinus Nijhoff, The Hague, Netherlands, 1983. □